A New Generation of Radiofluorinated Pyrimidine-2,4,6-triones as MMP-Targeted Radiotracers for Positron Emission Tomography

Daniela Schrigten,[†,‖] Hans-Jörg Breyholz,[†] Stefan Wagner,[†] Sven Hermann,[§] Otmar Schober,[†] Michael Schäfers,[§,‖] Günter Haufe,[‡] and Klaus Kopka*[,†,‖]

[†]Department of Nuclear Medicine, University Hospital Münster, Albert-Schweitzer-Campus 1, Building A1, D-48149 Münster, Germany

[‡]Organisch-Chemisches Institut, Westfälische Wilhelms-Universität, Corrensstrasse 40, D-48149 Münster, Germany

[§]European Institute for Molecular Imaging, University of Münster, Mendelstrasse 11, D-48149 Münster, Germany

[‖]Interdisciplinary Centre of Clinical Research (IZKF), Münster, Germany

S Supporting Information
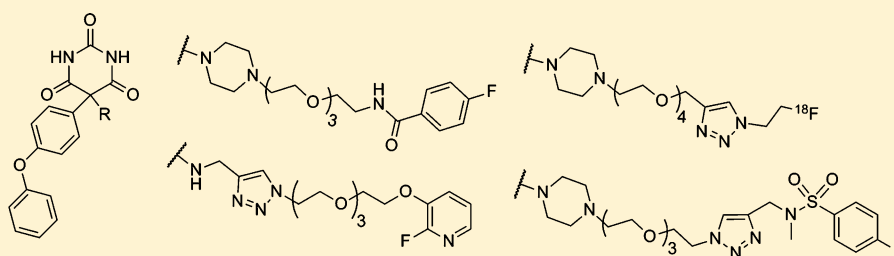
ABSTRACT: Radiolabeled C-5-disubstituted pyrimidine-2,4,6-triones have recently been suggested by our group as a class of potent matrix metalloproteinase (MMP) targeted radiotracers that can noninvasively visualize activated MMPs by means of positron emission tomography (PET). MMPs belong to the zinc- and calcium-dependent endopeptidases which are involved in the proteolytic degradation of components of the extracellular matrix (ECM) but also are capable of processing and releasing bioactive molecules such as growth factors, proteinase inhibitors, and cytokines. Locally increased levels of activated MMPs modulate and contribute to the progression of various diseases, such as cancer, atherosclerosis, stroke, arthritis, and others. Therefore, activated MMPs are suitable biological targets for the specific and noninvasive visualization of aforementioned pathologies in vivo. On the basis of our recent results, we here describe a series of new fluorinated pyrimidine-2,4,6-triones of the second generation with maintained MMP inhibition potencies (IC_{50} = 4−605 nM), which are fine-tuned toward more hydrophilic versions, and show the improved biodistribution behavior of one selected radiofluorinated pyrimidine-2,4,6-trione by means of small-animal PET.

■ INTRODUCTION

The visualization of locally up-regulated and activated extracellular matrix (ECM) degrading peptidases in vivo (such as matrix metalloproteinases (MMPs)) is a clinical challenge. MMPs are involved in the proteolytic degradation of ECM components but also are capable of modulating and initiating the release of bioactive molecules such as growth factors, proteinase inhibitors, and cytokines.[1] To date, more than 20 human MMPs have been characterized. On the basis of their specificity, the MMPs are classified into collagenases, gelatinases, stromelysins, and matrilysins. Another subclass of the MMPs is represented by the membrane-type MMPs (MT-MMPs) that additionally contain a transmembrane and intracellular domain, a membrane linker domain or are membrane associated.[2,3]

MMPs are secreted as inactive zymogens (pro-MMPs). Once activated via the "cysteine switch" mechanism, a zinc active site is provided that initiates its proteolytic activity.[4] Activated MMPs are tightly controlled by several endogenous inhibitors, e.g., the plasma inhibitor α_2-macroglobulin, four tissue inhibitors of metalloproteinases (TIMPs),[5] or the plasma-membrane anchored cell surface receptor RECK (reversion-inducing-cysteine-rich protein with kazal motifs).[6]

In pathophysiological processes an increased cytokine and growth factor-stimulated MMP gene transcription, followed by an abnormal pro-MMP secretion and zymogen activation, might become prevalent, triggering the progression of inflammation, cancer, or especially cardiovascular diseases like atherosclerosis and arterial aneurysm.[7,8]

There are several groups that are currently working on the development and evaluation of MMP inhibitor (MMPI) based radiotracers targeting MMPs in their activated forms and on the noninvasive imaging of MMP-associated diseases by means of single photon emission computed tomography (SPECT) or positron emission tomography (PET).[9−12]

Recently, the pyrimidine-2,4,6-triones (or barbiturates) were identified as potent MMPIs that exhibit specific activities by binding to the zinc(II) active site of a subgroup of activated MMPs comprising the gelatinases A (MMP-2) and B (MMP-9), neutrophil collagenase (MMP-8), and the membrane bound MMPs MT-1-MMP (MMP-14) and MT-3-MMP (MMP-16).[13] The C-5-disubstituted pyrimidine-2,4,6-trione derivative **1** (RO 28-2653) was found to exhibit a strong antitumoral and anti-angiogenic efficacy and thus is able to target tumor tissues.[14] These prerequisites support the approach of using the barbiturates as molecular MMP-targeted imaging agents.[15] In contrast to the bidentate zinc(II) binding moiety of the radiofluorinated hydroxamate-based MMP-targeted radiotracers recently introduced by our group,[16−18] it is speculated that the enolic tautomer of the pyrimidine-2,4,6-triones either binds in an almost tridentate manner to the zinc active site[19] or chelates in a monodentate pattern via a nitrogen whereupon the flanking oxygen atoms occupy the second coordination shell.[20]

We lately have introduced a first radiofluorinated C-5-disubstituted prototype MMP-targeted radiotracer, a potent and moderately lipophilic MMPI radiotracer based on the lead structure **1** (experimental log D of 2.15) showing one- to two-digit nanomolar IC_{50} values especially for the gelatinases (MMP-2, IC_{50} = 23 nM; MMP-9, IC_{50} = 7 nM) and which is radiolabeled with the prominent PET-compatible positron emitter ^{18}F (Figure 1).[21]
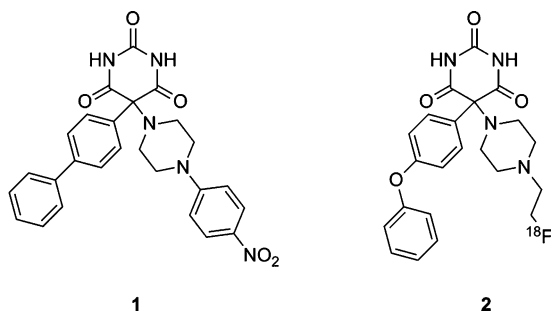

Figure 1. Structures of **1** (RO 28-2653) and radiofluorinated pyrimidine-2,4,6-trione of the first generation **2**.[21]

As expected, the preliminary biodistribution studies using the quadHIDAC small-animal PET device showed that this ^{18}F-labeled pyrimidine-2,4,6-trione does not specifically accumulate in tissues of nondiseased wild-type mice. The wholebody dynamic small-animal PET scan over 120 min indicated that the tracer uptake in nontarget organs, such as the brain, lung, heart, and muscle, was low over all time points. There was also a notable uptake in the bladder, indicative of a predominant renal excretion with some hepatobilliary clearance. In the case of occurring MMP-associated diseases the visualization of dysregulated MMP activity in possible target tissues such as brain, heart, lung, and tumors might be feasible. However, the clearance of any ^{18}F-labeled radiotracer candidate from a living subject should correspond with or be less than the physical half-life of the applied PET radionuclide (^{18}F, $T_{1/2}$ = 109.7 min), and thus, an excretion behavior of the radiotracer is desired that is more rapid compared with the ^{18}F-labeled prototype pyrimidine-2,4,6-trione to finally obtain high signal-to-noise ratios of detected target tissues within a shorter time frame.

We here present a series of new fluorinated pyrimidine-2,4,6-triones, fine-tuned with mini-polyethylene glycol (PEG) and

1,2,3-triazole building blocks in combination with known (radio)fluorinated prosthetic groups. As a result, a set of new MMPIs with very high MMP inhibition potencies covering a wide range of lipophilicities were synthesized. Hereupon we identified a radiofluorinated, more hydrophilic pyrimidine-2,4,6-trione of the second generation and discovered, by means of small-animal PET imaging, its significantly accelerated in vivo excretion characteristics compared with the radiofluorinated MMP-targeted radiotracer of the first generation.

■ RESULTS AND DISCUSSION

Chemistry. The pyrimidine-2,4,6-trione **1** was chosen as lead compound, and modifications were made in the piperazinyl moiety with the aim to improve the clearance characteristics and to enable ^{18}F-labeling while retaining MMP inhibition potencies of the resulting derivatives. This approach involves the introduction of short PEG chains, which are known to increase the hydrophilicity and the water solubility, directing the tracer to a predominant renal excretion route. Compared to a non-PEGylated derivative the mini-PEG tracer should therefore lead to a higher tracer-related signal-to-noise-ratio in the target tissue.[22−24] In addition we recently observed that by introduction of mini-PEG units as linkers at the piperazinyl moiety, the MMP inhibition potencies of modified barbiturate derivatives are maintained.[21,25]

The preparation of the key intermediates **8−12** is summarized in Scheme 1. Pyrimidine-2,4,6-triones **9**, **11**, and **12** were synthesized from the corresponding piperazines as previously reported by our group.[21,25] According to this procedure, the alkyne derivative **8** was prepared by reaction of 5-(4-phenoxyphenyl)pyrimidine-2,4,6-trione **3**[26] with propargyl-amine. Similarly, the piperazine **5** yielded the alkyne derivative **10** with an elongated PEG chain. To obtain the piperazine derivative **5** from tetraethylene glycol (TEG) (Scheme 2), a "Williamson type" coupling reaction[27] using potassium *tert*-butoxide (*t*-BuOK) in *tert*-butanol (*t*-BuOH) was applied affording the PEG$_8$ derivative **16** in 83% yield.

Next, a variety of fluorinated building blocks were incorporated into the pyrimidine-2,4,6-trione structure to give access to products with a wide range of lipophilicities and to fathom the tolerance to heterocycles in this position, in particular to 1,2,3-triazoles and fluoropyridinyl substituents. The lipophilic MMPI structures **13** and **14** were obtained as outlined in Scheme 1. Compound **14** was prepared in 78% yield via coupling with *N*-succinimidyl-4-fluoro-benzoate[28] in the presence of triethylamine.

A set of more hydrophilic pyrimidine-2,4,6-triones were achieved from alkyne- and azido-substituted intermediates **8−11** by employing copper(I) catalyzed 1,3-dipolar cycloadditions.[29] The fluorinated triazoles **28−36** were prepared in yields of 27−72% using copper(II) sulfate and sodium ascorbate in dimethylformamide (DMF) (Scheme 3). With an addition of the Cu(I)-stabilizing tris(benzyltriazolyl)methylamine ligand (TBTA), no improvement of reaction yields was observed.

These reaction pathways provided a novel series of pyrimidine-2,4,6-triones including nonradioactive reference compounds **13**, **14**, and **28−36** of potential ^{18}F-fluorinated radioligands as well as precursors **8−12** applicable for ^{18}F-labeling in two steps using the corresponding radiofluorinated prosthetic groups, e.g., *N*-succinimidyl-4-[^{18}F]fluorobenzoate ([^{18}F]SFB) for amino precursor **12**, 2-[^{18}F]fluoroethylazide for alkyne precursors **9** and **10**, and 2-[^{18}F]fluoro-3-(hex-5-ynyloxy)-pyridine ([^{18}F]FPy5yne) for azide precursor **11**.

In Vitro Enzyme Assays and log D Values. The IC_{50} values of the target compounds **13**, **14**, and **28−36** against

Scheme 1. Syntheses of Phenoxyphenylpyrimidine-2,4,6-triones 8−14[a]
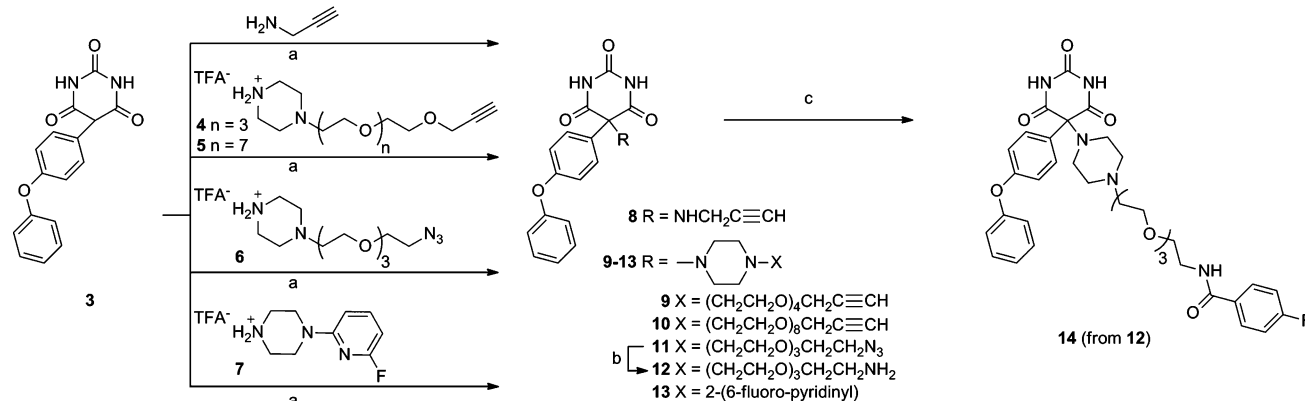
[a]Reaction conditions: (a) (1) NBS, DMF, 5−10 °C; (2) propargylamine or piperazines **4−7**, K_2CO_3, room temp, 18 h; (b) (1) PPh_3, THF, room temp, 16 h; (2) H_2O, room temp, 3 h; (c) *N*-succinimidyl-4-fluorobenzoate, Et_3N, CH_2Cl_2, room temp, 7.5 h.

Scheme 2. Synthesis of Piperazine 5[a]
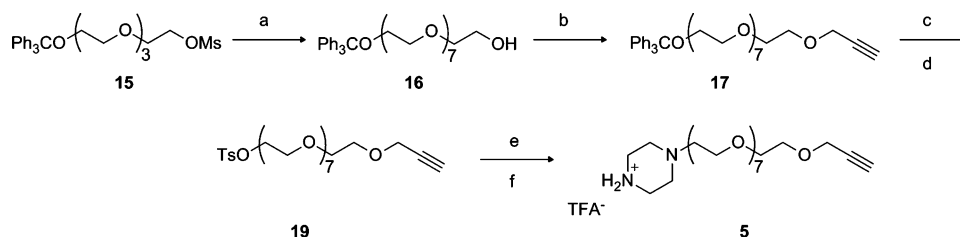
[a]Reaction conditions: (a) TEG, *t*-BuOK, *t*-BuOH, reflux, 18 h; (b) propargyl bromide, NaH, THF, 0 °C, then room temp, 26 h; (c) TsOH·H_2O, MeOH, reflux, 20 h; (d) TsCl, Et_3N, CH_2Cl_2, 0 °C, then room temp, 18 h; (e) 1-Boc-piperazine, Et_3N, CH_3CN, reflux, 24 h; (f) TFA, CH_2Cl_2, room temp, 19 h.

activated MMP-2, -8, -9, and -13 were measured by fluorogenic in vitro inhibition assays following the procedure previously described.[30] The assays were validated using the nonradioactive versions of the MMP inhibitors. IC_{50} values were obtained from nonlinear regression analysis of the concentration-dependent reaction rates.

As displayed in Table 1, the target compounds revealed, similar to the previously reported (radio)ligand **2**, MMP inhibition potencies in the nanomolar range (IC_{50} of 4−605 nM). These results clearly demonstrate a wide tolerance to modifications at the piperazinyl moiety, which orients into the S_2' subsite of the activated MMP. The modifications include insertion of 1,2,3-triazoles and fluoropyridinyl substituents. Moreover, as a new finding, replacement of the piperazinyl moiety gave MMPIs **28** and **29** with inhibition potencies comparable to those of derivatives comprising this group. We have selected compounds **28** and **29**, avoiding the piperazinyl approach but mimicking the nitrogen−nitrogen distance given in the piperazinyl moiety.

Because of the fact that the hydrophilicity of a radioligand has a significant impact on the biodistribution characteristics of any radiotracer, an evaluation of the hydrophilic properties of the target compounds is required. Therefore, the corresponding calculated log *D* values (clogD) were tabulated along with the inhibition potencies (Table 1). The obtained new generation of pyrimidine-2,4,6-triones shows clogD values ranging from −0.45 (MMPI **31**) to 4.27 (MMPI **13**). The differing log *D* values display the influence of the incorporation of structural features such as PEG units and 1,2,3-triazoles in combination with fluorinated building blocks.

Additionally, the partition coefficient (log *D*) of the radio-fluorinated analog [^{18}F]**30** (see section Radiochemistry) was determined experimentally (log *D* (exp) = 0.78 ± 0.02). The experimental log *D* is comparable to the calculated value (clogD (**30**) = 0.99). The pyrimidine-2,4,6-trione **30** is therefore approximately 100 times more hydrophilic than the first generation radioligand **2**. The desired increased hydrophilicity of pyrimidine-2,4,6-trione **30** is indeed realized while maintaining its in vitro MMP inhibition characteristics, as shown by the double-digit nanomolar IC_{50} values. This encouraged us to further improve the radiosynthesis of the ^{18}F-labeled isotopolog [^{18}F]**30**, as follows, aiming at initial in vivo experiments using this new MMPI radiotracer.

Radiochemistry. The 2-[^{18}F]fluoroethylazide-conjugated pyrimidine-2,4,6-trione [^{18}F]**30** was achieved by a semi-automated two-step procedure consisting of the nucleophilic radiofluorination of 2-azidoethyl-4-methylbenzenesulfonate[31] and subsequent copper(I) catalyzed cycloaddition with the alkyne precursor **9** (Scheme 4). The radiosynthesis of click chemistry building block 2-[^{18}F]fluoroethylazide ([^{18}F]**24**) was carried out according to a procedure previously described by Glaser and Årstad.[32] [^{18}F]**24** could be isolated by distillation in 68 ± 8% radiochemical yields (decay corrected, *n* = 6). The click labeling was performed outside the automated synthesizer. Investigations of the impact of reaction time, temperature, and the catalytic system on the radiochemical yield of [^{18}F]**30** revealed the optimal conditions to be 8 min of reaction time at room temperature in the presence of 2 equiv of copper sulfate relative to the alkyne precursor **9**. This successfully provided the 1,4-disubstituted 1,2,3-triazole [^{18}F]**30** in radiochemical

Scheme 3. Syntheses of 1,2,3-Triazoles 28−36[a]
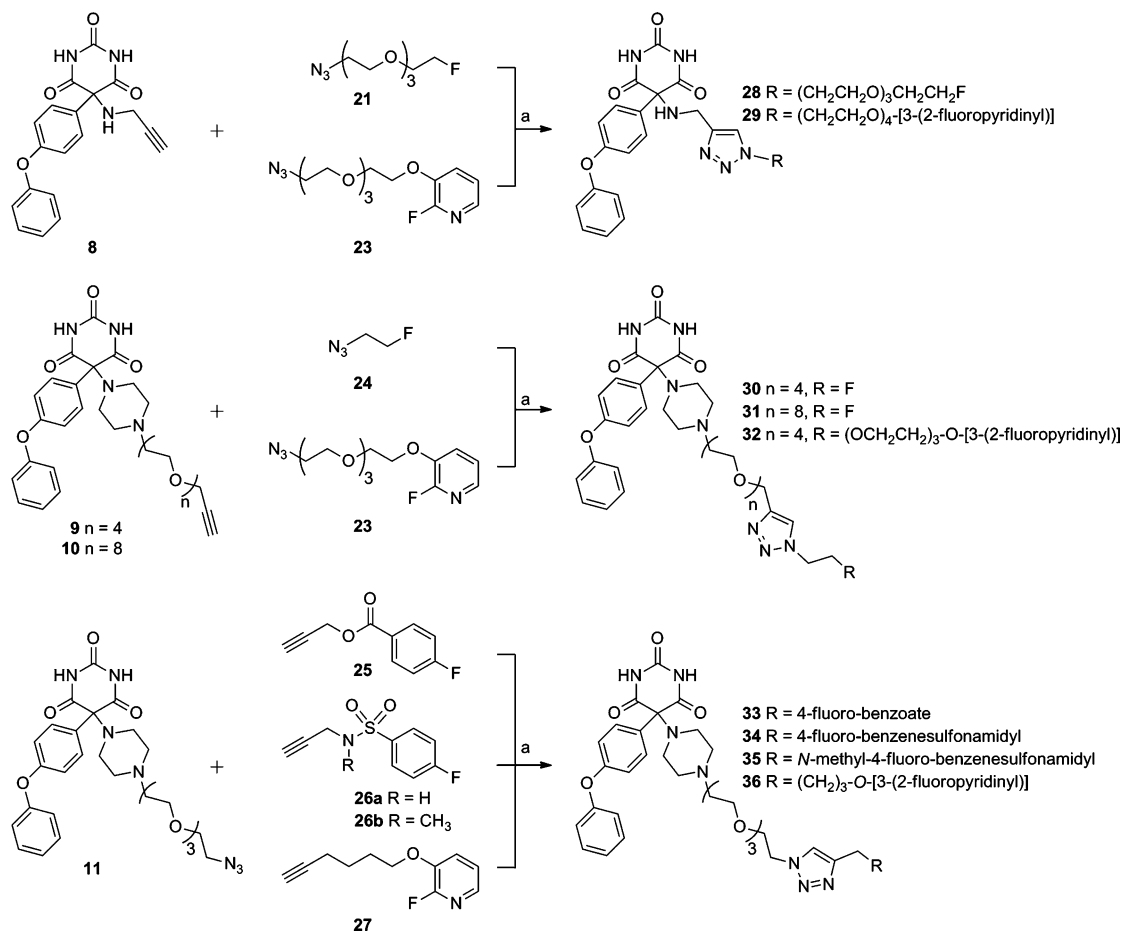
[a]Reaction conditions: (a) CuSO$_4$·5H$_2$O, sodium ascorbate, DMF, room temp, 2.5−72 h.

**Table 1. IC$_{50}$ and log D of Novel Pyrimidine-2,4,6-triones 13, 14, and 28−36**

| compd | IC$_{50}$ (nM)[a] | | | | log D | |
	MMP-2	MMP-8	MMP-9	MMP-13	clogD[b]	log D (exp)
2	23 ± 9	138 ± 12	7 ± 2	645 ± 17	2.88	2.15 ± 0.02[21]
13	203 ± 47	129 ± 28	9 ± 2	48 ± 13	4.27	
14	5 ± 2	15 ± 6	4 ± 0.2	16 ± 3	3.24	
28	64 ± 7	48 ± 4	41 ± 2	87 ± 7	1.07	
29	29 ± 10	49 ± 36	10 ± 1	9 ± 1	1.80	
30	58 ± 14	58 ± 3	27 ± 6	51 ± 11	0.99	0.78 ± 0.02[c]
31	44 ± 3	150 ± 21	74 ± 19	94 ± 58	−0.45	
32	202 ± 25	107 ± 38	56 ± 25	605 ± 16	0.82	
33	22 ± 9	27 ± 1	23 ± 7	7 ± 1	3.09	
34	13 ± 0.2	19 ± 1	20 ± 3	23 ± 2	2.09	
35	12 ± 1	15 ± 0.2	7 ± 1	21 ± 7	2.59	
36	52 ± 4	116 ± 17	60 ± 20	40 ± 13	3.23	

[a]Values are the mean ± SD of three experiments. [b]clogD values were calculated by ACD/Chemsketch, version 6.00, ACD/Laboratories (log D = log P at physiological pH (7.4)). [c]log D value was determined for compound [^{18}F]30. Value is the mean ± SD of two independent experiments.

yields of 63 ± 10% (decay-corrected, n = 6). After purification by semipreparative HPLC, concentration by rotary evaporation, and formulation, the two-step radiosynthesis of [^{18}F]30 was accomplished with an overall radiochemical yield of 43 ± 9% (decay corrected, n = 6) in 140 min from the end of radionuclide production. The radiochemical purity of [^{18}F]30 was >97%, and the determined specific activities were 11−20 GBq·μmol^{-1} at the end of radiosynthesis. The radioligand was

formulated in phosphate buffered saline (PBS) to determine log D$_{7.4}$ values and to study its in vitro stability in human serum at 37 °C.

In Vitro Stability. An in vitro stability study was carried out using human serum. During long-term incubation for up to 120 min at 37 °C, [^{18}F]30 revealed an excellent stability. As shown in Figure 2, only parent compound [^{18}F]30 can be detected by radio-HPLC. Radiometabolites cannot be observed.

Scheme 4. Radiosynthesis of 2-[^{18}F]Fluoroethylazide-Conjugated Pyrimidine-2,4,6-trione [^{18}F]30[a]
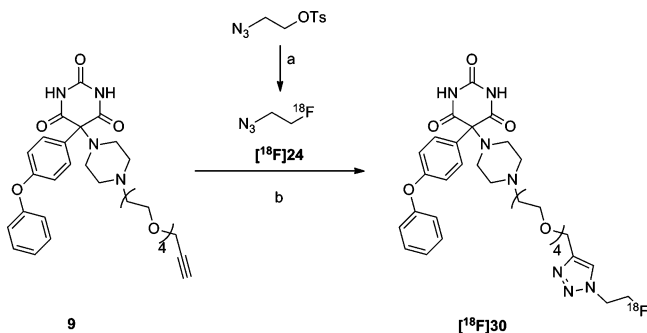
[a]Reaction conditions: (a) [^{18}F]fluoride (potassium 222 cryptate), K$_2$CO$_3$, CH$_3$CN, 84 °C, 15 min; (b) CuSO$_4$·H$_2$O, sodium ascorbate, DMF, room temp, 8 min.
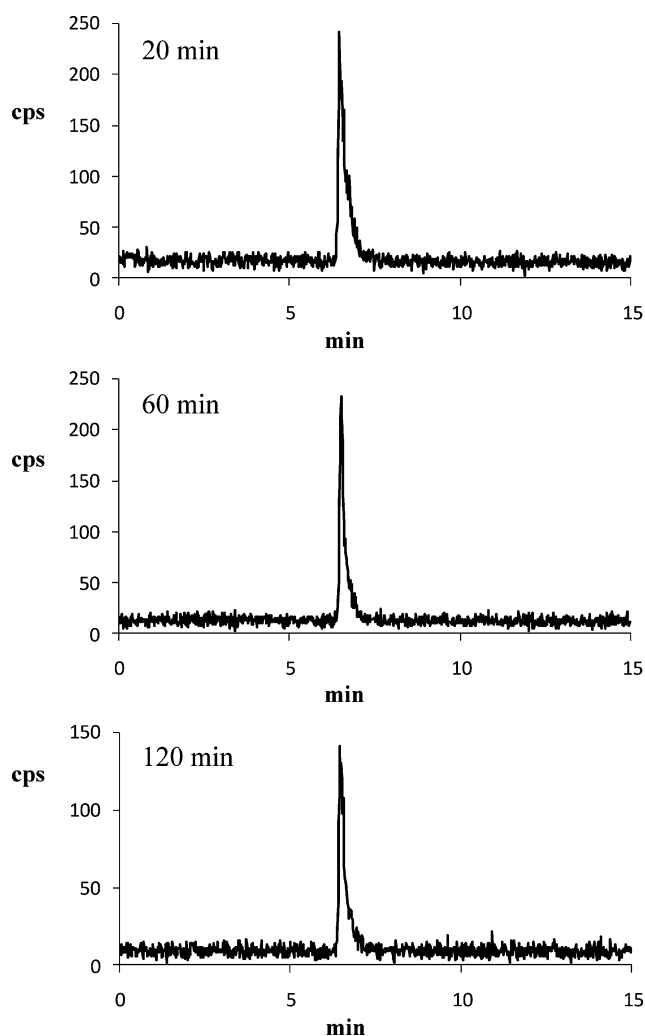

Figure 2. Stability of [^{18}F]30 (t_R = 6.5 min; analytical HPLC system II, linear gradient from 10% to 90% CH$_3$CN in water (0.1% TFA) over 9 min, followed by a linear gradient from 90% to 10% CH$_3$CN in water (0.1% TFA) over 6 min, 1.5 mL·min^{-1}) after incubation in human serum in vitro at 37 °C after 20 min (top), 90 min (middle), and 120 min (bottom).

In Vivo Biodistribution Study. Biodistribution characteristics of radiotracer [^{18}F]30 were studied in adult Balb/c mice. Dynamic PET scans, co-registered to computed tomography

(CT), were performed throughout the studies and reconstructed into a series of images reflecting the radiotracer distribution at different time frames after injection of [^{18}F]30 (Figure 3).
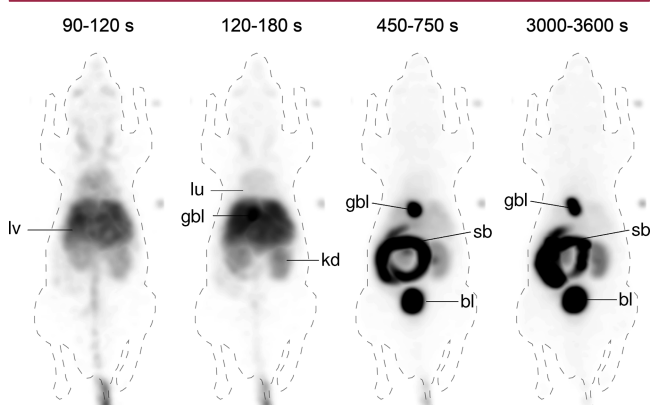

Figure 3. Biodistribution of radioactivity in adult C57/BL6 mouse after intravenous injection of [^{18}F]30 visualized by small-animal PET. Images represent maximum intensity projections at selected time frames. Labeled structures are as follows: liver (lv), gallbladder (gbl), bladder (bl), kidneys (kd), small bowel (sb), lung (lu).

A similar pharmacokinetic behavior was observed compared to radioligand **2** which has been described earlier by our group.[21] The tracer uptake in nontarget organs, such as brain, heart, and lung, was low over all time points. Furthermore, low accumulation of [^{18}F]30 in the skeleton suggests that the extent of tracer defluorination and generation of free [^{18}F]fluoride was negligible. [^{18}F]30 is notably excreted via the kidneys and the liver as indicated by the tracer accumulation in the urinary bladder and the gallbladder/intestine, respectively. For tissues involved in metabolic and excretory processes (liver, gallbladder, intestine, kidney, bladder) and for potential regions for diagnostic MMP-PET, CT-guided volumes of interest (VOIs) were defined and time−activity curves were determined (Figure 4).

Initially, a high level of radioactivity is observed in the liver which decreases to background level in 10−15 min pi. In comparison, model tracer **2** features a much slower clearance from the liver in 90−120 min pi. Furthermore, by comparison of the renal elimination of model tracer **2** with the more hydrophilic radioligand [^{18}F]30, the latter presents a faster clearance from the kidneys. Hence, alteration of the chemical structure by introducing a mini-PEG and a triazole unit led to a favorable pharmacokinetic behavior for in vivo PET-imaging.

■ CONCLUSION

Extending our recent work on the development of MMP-targeted radioligands, we herein present the synthesis and in vitro characterization of a new series of fluorinated pyrimidine-2,4,6-trione-based MMPIs derived from lead structure **1**. All compounds were evaluated as potent inhibitors of MMP-2, -8, -9, and -13 with calculated log D values ranging from −0.45 to 4.27. This allows a systematic investigation of the effect of hydrophilicity on biodistribution patterns of respective radiofluorinated PET tracers together with the exploration of their in vivo stability. One promising MMPI, [^{18}F]30, with an increased hydrophilicity compared to model tracer **2** described earlier by our group,[21] was successfully radiolabeled with good radiochemical yields of 43 ± 9%. This radiofluorinated pyrimidine-2,4,6-trione [^{18}F]30 of the new generation revealed an excellent serum
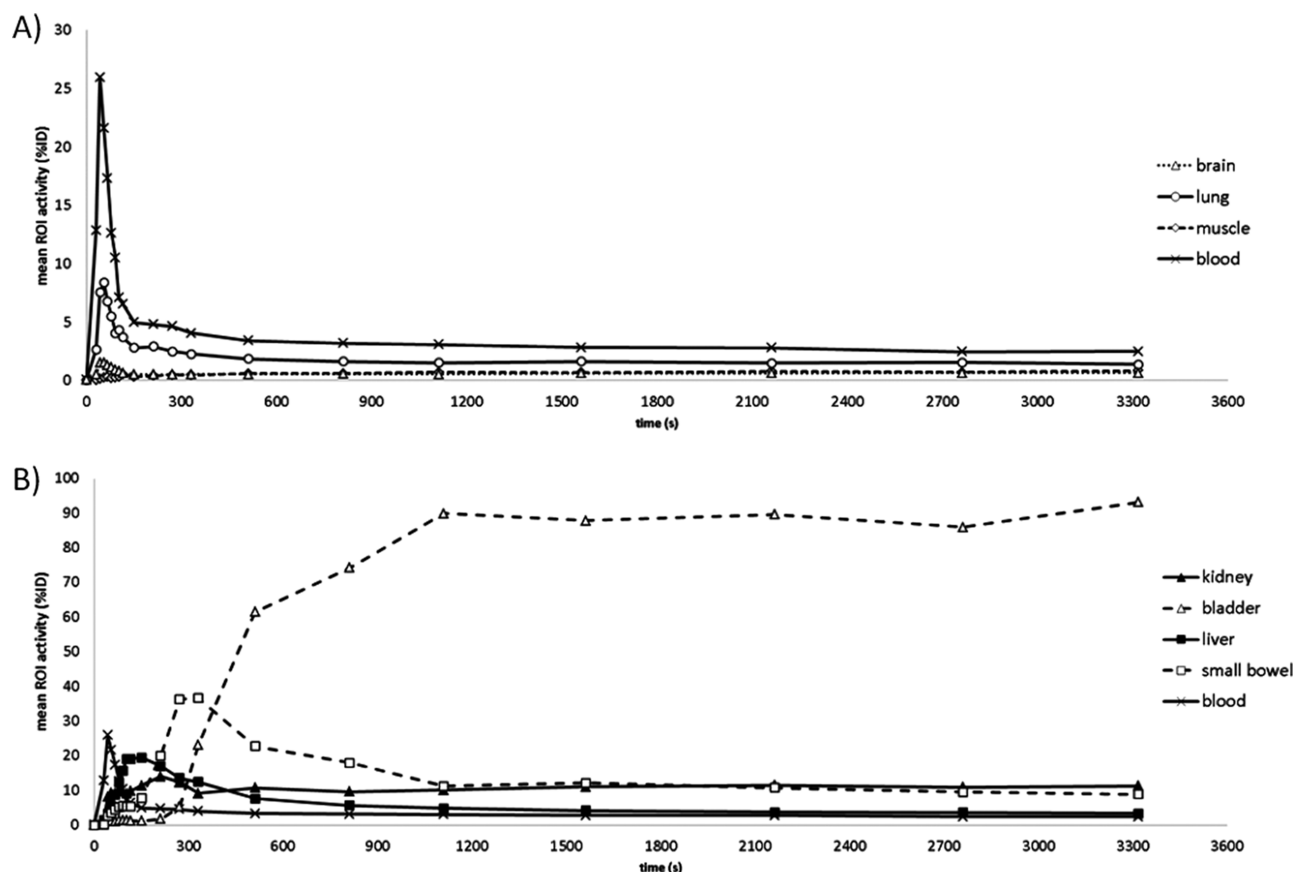
Figure 4. Representative biodistribution of radioactivity in adult C57/Bl6 mouse after intravenous injection of [^{18}F]**30**: (A) time—activity curves of the blood, brain, lung, and muscle; (B) time—activity curves of blood, kidney, bladder, liver, and small bowel; ROI, region of interest; % ID, percent injected dose.

stability in vitro and more rapid clearance characteristics, as shown by in vivo biodistribution studies in wild type mice. Thus, [^{18}F]**30** represents a promising MMP-targeted radiotracer for the noninvasive PET imaging of activated MMPs in vivo, which is putatively more favorable compared to compound **2** with respect to the physical half-life of the PET-radionuclide ^{18}F. In the next step preclinical PET/CT studies in disease models with known MMP up-regulation (e.g., tumor, Lewis lung carcinoma bearing mice; atherosclerotic plaques, apolipoprotein E-deficient mice) will be assessed.

■ EXPERIMENTAL SECTION

General. All chemicals, reagents, and solvents were analytical grade, purchased from commercial suppliers, and used without further purification unless otherwise specified. Melting points were measured on a Stuart Scientific SMP3 capillary melting point apparatus and are uncorrected. ^{1}H NMR, ^{13}C NMR, and ^{19}F NMR spectra were recorded in CDCl$_3$ or in DMSO-d_6 on Bruker AV400, Bruker AV300, or Varian Unity plus 600 spectrometer with the corresponding solvent signals as an internal standard. For ^{19}F NMR shift values, CFCl$_3$ was the internal standard. Chemical shifts are reported in δ (ppm). Exact mass analyses were conducted on a Bruker MicroTof apparatus. Reactions were monitored by thin layer chromatography (TLC, performed on silica gel coated polyester backed TLC plates, SIL G/UV$_{254}$, Macherey-Nagel) using solvent mixtures of cyclohexane (CH), ethyl acetate (EtOAc), methanol (MeOH), and triethylamine (TEA). The ≥95% purities of each new nonradioactive compound were assessed by elementary analysis or analytical reversed phase HPLC on HPLC system I: two Smartline 1000 pumps and a Smartline UV detector 2500 (Knauer), a GabiStar γ-detector (Raytest Isoto-penmessgeräte GmbH), and a Nucleosil Eurosphere 100-5 C-18

column (250 mm × 4.6 mm). The recorded data were processed by the GINA Star software (Raytest Isotopenmessgeräte GmbH). The HPLC system I started with a linear gradient from 10% to 90% CH$_3$CN in water (0.1% TFA) over 9 min, followed by a linear gradient from 90% to 10% CH$_3$CN in water (0.1% TFA) over 6 min, with a flow rate of 1 mL·min^{-1} (unless otherwise specified). N-Boc piperazine, pyrimidine-2,4,6-triones **4**, **6**, and **12**, and PEG derivatives **15** and **21** were prepared as previously described by our group.[21,25] The syntheses of 5-(4-phenoxyphenyl)pyrimidine-2,4,6-trione,[26] N-succinimidyl-4-fluorobenzoate,[25] 2-azidoethyl-4-methylbenzenesul-fonate,[31] 2-fluoroethylazide (**24**),[32] propargyl 4-fluorobenzoate (**25**),[33] and 4-fluoro-N-methyl-N-(prop-2-ynyl)benzenesulfonamide (**26b**)[34] were carried out according to literature procedures. 4-(6-Fluoropyridin-2-yl)piperazin-1-ium trifluoroacetate (**7**) was prepared from 4-(6-fluoropyridin-2-yl)piperazine-1-carboxylic acid *tert*-butyl ester[35] via deprotection with trifluoroacetic acid (TFA). 4-Fluoro-3-(hex-5-ynyloxy)pyridine (**27**) was synthesized as described by Inkster et al.[36] According to this procedure, 3-(2-{2-[2-(2-azidoethoxy)-ethoxy]ethoxy}ethoxy)-2-fluoropyridine (**23**) was prepared from toluene-4-sulfonic acid 2-{2-[2-(2-azidoethoxy)ethoxy]ethoxy}ethyl ester[21] (see Supporting Information). All animal experiments were conducted in accordance with local institutional guidelines for the care and use of laboratory animals.

General Procedure for the Preparation of Pyrimidine-2,4,6-triones 8, 10, and 13. Compounds **8**, **10**, and **13** were synthesized according to previously described procedures.[25,26] A solution of 5-(4-phenoxyphenyl)pyrimidine-2,4,6-trione (2—10 mmol, 1 equiv) in DMF (2 mL/mmol) was cooled to 10 °C, and a solution of NBS (2—10 mmol, 1 equiv) in DMF (1 mL/mmol) was added dropwise. After the mixture was stirred at 5—10 °C for 20 min, propargylamine (10 mmol, 1 equiv), compound **5** (2 mmol, 1 equiv), or compound **7** (2.5 mmol, 1 equiv) was added in one portion, followed by potassium

carbonate (4−20 mmol, 2 equiv). After being stirred for 1 h at 5−10 °C, the mixture was allowed to warm to room temperature and then stirred overnight.

5-(4-Phenoxyphenyl)-5-prop-2-ynylaminopyrimidine-2,4,6-trione (8). For the preparation of **8**, 5-(4-phenoxyphenyl)pyrimidine-2,4,6-trione (2.96 g, 10.0 mmol) and propargylamine (640 μL, 551 mg, 10.0 mmol) were subjected to the general procedure. For workup, the reaction mixture was poured onto ice−water and adjusted to pH 4, using dilute hydrochloric acid (6 N). The resulting precipitate was filtered off, stirred in diethyl ether, and dried in vacuo, giving **8** as an off-white solid (1.73 g, 50%). Mp: 248−249 °C (dec). ^{1}H NMR (300 MHz, DMSO-d_6): δ 3.17 (t, 1H, ^4J = 1.7 Hz, C≡CH), 3.34 (br s, 1H, NH), 3.38−3.46 (m, 2H, NH−CH_2), 6.99−7.05 (m, 4H, H$_{Aryl}$), 7.14−7.20 (m, 1H, H$_{Aryl}$), 7.37−7.46 (m, 4H, H$_{Aryl}$), 11.65 (br s, 2H, NH) ppm. ^{13}C NMR (75.5 MHz, DMSO-d_6): δ 33.54, 68.78, 75.40, 81.64, 118.31, 119.15, 124.00, 128.11, 130.18, 132.42, 149.73, 155.93, 157.29, 170.64 ppm. HRMS-ESI: calcd for C$_{19}$H$_{15}$N$_3$O$_4$Na ([M + Na]$^+$), 372.0955; found 372.0955. The purity of **8** was determined by analytical HPLC to be 96%, t_R = 7.90 ± 0.02 min (n = 3).

5-(4-Phenoxyphenyl)-5-{4-[2-(2-{2-[2-(2-{2-[2-(2-prop-2-ynyloxy-ethoxy)ethoxy]ethoxy}ethoxy)ethoxy]ethoxy}ethoxy)ethyl]piper-azin-1-yl}pyrimidine-2,4,6-trione (10). For the preparation of **10**, 5-(4-phenoxyphenyl)pyrimidine-2,4,6-trione (593 mg, 2 mmol) and **5** (1.18 g, 2 mmol) were subjected to the general procedure. For workup, the reaction mixture was diluted with EtOAc, followed by addition of aqueous citric acid (0.1 mmol mL^{-1}). After separation of the organic phase, the aqueous phase was extracted with EtOAc (2×). The combined organic extracts were washed with water, dried (MgSO$_4$), filtered, and concentrated. The residue was purified by silica gel chromatography (EtOAc/MeOH, 4/1) to afford **10** as a waxy oil (1.23 g, 80%). ^{1}H NMR (400 MHz, CDCl$_3$): δ 2.43 (t, 1H, ^4J = 2.4 Hz, C≡CH), 2.74−2.81 (m, 10H, N−CH_2), 3.56−3.69 (m, 30H, CH_2), 4.18 (d, 2H, ^4J = 2.4 Hz, CH_2−C≡CH), 6.94−6.96 (m, 2H, H$_{Aryl}$), 7.00−7.02 (m, 2H, H$_{Aryl}$), 7.11−7.16 (m, 1H, H$_{Aryl}$), 7.32−7.36 (m, 2H, H$_{Aryl}$), 7.46−7.48 (m, 2H, H$_{Aryl}$). ^{13}C NMR (101 MHz, CDCl$_3$): δ 46.95, 53.64, 57.40, 58.49, 67.54, 69.18, 70.41, 70.43, 70.47, 70.50, 70.51, 70.53, 70.56, 70.58, 70.59, 70.60, 70.64, 74.31, 74.76, 79.78, 118.36, 119.66, 124.05, 128.83, 130.01, 130.12, 149.40, 156.40, 158.38, 169.70 ppm. HRMS-ESI: calcd for C$_{39}$H$_{54}$N$_4$O$_{12}$ ([M + H]$^+$), 771.3811; found 771.3809. The purity of **10** was determined by analytical HPLC to be 98%, t_R = 8.12 ± 0.01 min (n = 3).

5-[4-(6-Fluoropyridin-2-yl)piperazin-1-yl]-5-(4-phenoxyphenyl)pyrimidine-2,4,6-trione (13). For the preparation of **13**, 5-(4-phenoxyphenyl)pyrimidine-2,4,6-trione (741 mg, 2.50 mmol) and **7** (736 mg, 2.50 mmol) were subjected to the general procedure. For workup, the reaction mixture was diluted with EtOAc, followed by an addition of aqueous citric acid (0.1 mmol mL^{-1}). After separation of the organic phase, the aqueous phase was extracted with EtOAc (2×). The combined organic extracts were washed with water, dried (MgSO$_4$), filtered, and concentrated. The residue was purified by silica gel chromatography (CH/EtOAc, 2/1) and the concentrated eluent was subsequently stirred in diethyl ether to afford **13** as a white solid (812 mg, 68%). Mp: 235 °C. ^{1}H NMR (600 MHz, DMSO-d_6): δ 2.67−2.69 (m, 4H, N−CH_2), 3.45−3.47 (m, 4H, N−CH_2), 6.26 (dd, 1H, ^3J = 7.7 Hz, ^4J = 2.8 Hz, H$_{Pyridinyl}$), 6.63 (dd, 1H, ^3J = 8.3 Hz, ^4J = 2.5 Hz, H$_{Pyridinyl}$), 7.03−7.09 (m, 4H, H$_{Aryl}$), 7.17−7.20 (m, 1H, H$_{Aryl}$), 7.40−7.47 (m, 4H, H$_{Aryl}$), 7.60−7.69 (m, 1H, H$_{Pyridinyl}$), 11.66 (br s, 2H, NH) ppm. ^{13}C NMR (75.5 MHz, DMSO-d_6): δ 45.29, 47.29, 74.17, 95.34 (d, ^2J = 37 Hz), 103.48 (d, ^4J = 3.2 Hz), 118.20, 119.40, 124.17, 129.44, 129.67, 130.23, 142.62 (d, ^3J = 8.0 Hz), 149.41, 155.74, 157.60, 157.88 (d, ^3J = 15.9 Hz), 162.02 (d, ^1J = 233 Hz), 169.98 ppm. ^{19}F NMR (282 MHz, DMSO-d_6): δ −68.70 ppm. HRMS-ESI: calcd for C$_{25}$H$_{22}$FN$_5$O$_4$ ([M + H]$^+$), 476.1729; found 476.1724. Anal. Calcd for C$_{25}$H$_{22}$FN$_5$O$_4$: C 63.15, H 4.66, N 14.73. Found: C 62.96, H 4.80, N 14.46.

4-Fluoro-N-(2-{2-[2-(2-{4-[2,4,6-trioxo-5-(4-phenoxyphenyl)-hexahydropyrimidin-5-yl]piperazin-1-yl}ethoxy)ethoxy]-ethoxy}ethyl)benzamide (14). TEA (0.1 mL, 0.72 mmol) was added to a solution of **12** (150 mg, 0.27 mmol) in CH$_2$Cl$_2$ (4 mL), followed by N-succinimidyl-4-fluorobenzoate (70 mg, 0.30 mmol).

The mixture was stirred at room temperautre for 7.5 h and evaporated to dryness. The crude product was purified by silica gel chromatography (EtOAc/MeOH (9/1) + 2% TEA) to give pure **14** (143 mg, 78%). Mp: 124−126 °C. ^{1}H NMR (300 MHz, DMSO-d_6): δ 2.41−2.57 (m, 10H, N−CH_2), 3.35−3.53 (m, 14H, CH_2), 7.00−7.06 (m, 4H, H$_{Aryl}$), 7.14−7.20 (m, 1H, H$_{Aryl}$), 7.24−7.32 (m, 2H, H$_{Aryl}$), 7.37−7.44 (m, 4H, H$_{Aryl}$), 7.88−7.96 (m, 2H, H$_{Aryl}$), 8.55 (t, 1H, ^3J = 5.5 Hz, NH), 11.62 (br s, 2H, NH) ppm. ^{13}C NMR (75.5 MHz, DMSO-d_6): δ 43.37, 47.29, 53.72, 57.11, 68.11, 68.88, 69.64, 69.74, 73.95, 115.17 (d, ^2J = 21.6 Hz), 118.07, 119.29, 124.07, 129.65, 129.69, 129.82 (d, ^3J = 9.0 Hz), 130.19, 130.87 (d, ^4J = 2.8 Hz), 149.44, 155.81, 157.39, 163.82 (d, ^1J = 248 Hz), 165.18, 169.98 ppm. ^{19}F NMR (282 MHz, DMSO-d_6): δ −109.64 ppm. HRMS-ESI: calcd for C$_{35}$H$_{40}$FN$_5$O$_8$ ([M + H]$^+$), 678.2934; found 678.2935. Anal. Calcd for C$_{35}$H$_{40}$FN$_5$O$_8$: C 62.03, H 5.95, N 10.33. Found: C 61.63, H 5.85, N 10.31.

General Procedure for the Preparation of Triazoles 28−36. To a solution of the acetylene compound (0.5−1.0 mmol, 1 equiv) in DMF (8 mL·mmol^{-1}) were added aqueous CuSO$_4$·5H$_2$O (30−50 mol %), aqueous sodium ascorbate (40−60 mol %), and the corresponding azide (0.5−1.2 mmol, 1.0−1.2 equiv) in sequence. After the mixture was stirred at room temperature, the solvents were removed and the residue was purified by silica gel chromatography (EtOAc + 2% TEA → EtOAc/MeOH (4/1) + 2% TEA). ^{1}H, ^{13}C, and ^{19}F NMR data of triazoles **28−36** are listed in the Supporting Information.

5-{[1-(2-{2-[2-(2-Fluoroethoxy)ethoxy]ethoxy}ethyl)-1H-1,2,3-triazol-4-ylmethyl]amino}-5-(4-phenoxyphenyl)-pyrimidine-2,4,6-trione (28). For the preparation of **28**, **8** (349 mg, 1 mmol), CuSO$_4$·5H$_2$O (75 mg, 0.3 mmol, 30 mol %, in 1 mL of H$_2$O), sodium ascorbate (79 mg, 0.4 mmol, 40 mol %, in 1 mL of H$_2$O), and **21** (221 mg, 1 mmol) were subjected to the general procedure. After the mixture was stirred for 2.5 h, the reaction yielded **28** as an off-white foam (413 mg, 72%). Mp: 117 °C. HRMS-ESI: calcd for C$_{27}$H$_{31}$FN$_6$O$_7$ ([M + Na]$^+$), 593.2130; found 593.2138. Anal. Calcd for C$_{27}$H$_{31}$FN$_6$O$_7$: C 56.84, H 5.48, N 14.73. Found: C 56.47, H 5.43, N 14.53.

5-({1-[2-(2-{2-[2-(2-Fluoropyridin-3-yloxy)ethoxy]ethoxy}-ethoxy)ethyl]-1H-1,2,3-triazol-4-ylmethyl}amino)-5-(4-phenoxyphenyl)pyrimidine-2,4,6-trione (29). For the preparation of **29**, **8** (349 mg, 1 mmol), CuSO$_4$·5H$_2$O (100 mg, 0.4 mmol, 40 mol %, in 1 mL of H$_2$O), and sodium ascorbate (99 mg, 0.5 mmol, 50 mol %, in 1 mL of H$_2$O) and **23** (314 mg, 1 mmol) were subjected to the general procedure. After the mixture was stirred for 23 h, the reaction yielded **29** as a light yellow solid (438 mg, 66%). Mp: 104 °C. HRMS-ESI: calcd for C$_{32}$H$_{34}$FN$_7$O$_8$Na ([M + Na]$^+$), 686.2345; found 686.2346. The purity of **29** was determined by analytical HPLC to be 96%, t_R = 8.30 ± 0.03 min (n = 3).

5-(4-{2-[2-(2-{2-[1-(2-Fluoroethyl)-1H-1,2,3-triazol-4-ylmethoxy]ethoxy}ethoxy)ethoxy]ethyl}piperazin-1-yl)-5-(4-phenoxyphenyl)pyrimidine-2,4,6-trione (30). For the preparation of **30**, **9** (595 mg, 1 mmol), CuSO$_4$·5H$_2$O (75 mg, 0.3 mmol, 30 mol %, in 1 mL of H$_2$O), sodium ascorbate (79 mg, 0.4 mmol, 40 mol %, in 1 mL of H$_2$O), and a solution of **24** (107 mg, 1.2 mmol) were subjected to the general procedure. After stirring for 72 h, the reaction yielded **30** as a white solid (440 mg, 64%). Mp: 118 °C. HRMS-ESI: calcd for C$_{33}$H$_{42}$FN$_7$O$_8$ ([M + H]$^+$), 684.3152; found 684.3168. Anal. Calcd for C$_{33}$H$_{42}$FN$_7$O$_8$: C 57.97, H 6.19, N 14.34. Found: C 57.55, H 6.18, N 14.04.

5-[4-(2-{2-[2-(2-{2-[2-(2-{2-[1-(2-Fluoroethyl)-1H-1,2,3-tria-zol-4-ylmethoxy]ethoxy}ethoxy)-ethoxy]ethoxy}ethoxy)-ethoxy]ethyl}piperazin-1-yl]-5-(4-phenoxyphenyl)-pyrimidine-2,4,6-trione (31). For the preparation of **31**, **10** (385 mg, 0.5 mmol), CuSO$_4$·5H$_2$O (37 mg, 0.15 mmol, 30 mol %, in 0.5 mL of H$_2$O), sodium ascorbate (40 mg, 0.2 mmol, 40 mol %, in 0.5 mL of H$_2$O) and a solution of **24** (53 mg, 0.6 mmol) were subjected to the general procedure. After the mixture was stirred for 24 h, the reaction yielded **31** as a colorless oil (152 mg, 35%). HRMS-ESI: calcd for C$_{41}$H$_{59}$FN$_7$O$_{12}$ ([M + H]$^+$), 860.4200; found 860.4182. The purity of **31** was determined by analytical HPLC to be 95%, t_R = 7.62 ± 0.01 min (n = 3).

5-[4-(2-{2-[2-(2-{1-[2-(2-{2-[2-(2-Fluoropyridin-3-yloxy)-ethoxy]ethoxy}ethoxy)ethyl]-1H-1,2,3-triazol-4-ylmethoxy}-ethoxy)ethoxy]ethoxy}ethyl)piperazin-1-yl]-5-(4-phenoxyphenyl)pyrimidine-2,4,6-trione (32). For the preparation

of **32**, **9** (297 mg, 0.5 mmol), CuSO$_4$·5H$_2$O (37 mg, 0.15 mmol, 30 mol %, in 0.5 mL of H$_2$O), sodium ascorbate (40 mg, 0.2 mmol, 40 mol %), and **23** (157 mg, 0.5 mmol) were subjected to the general procedure. After the mixture was stirred for 2.5 h, the reaction yielded **32** as a colorless oil (284 mg, 62%). HRMS-ESI: calcd for C$_{44}$H$_{57}$FN$_8$O$_{12}$ ([M + H]$^+$), 909.4153; found 909.4158. The purity of **32** was determined by analytical HPLC to be 95%, t_R = 8.23 ± 0.01 min (n = 3).

4-Fluorobenzoic Acid 1-(2-{2-[2-(2-{4-[2,4,6-Trioxo-5-(4-phenoxyphenyl)hexahydropyrimidin-5-yl]piperazin-1-yl}-ethoxy)ethoxy]ethoxy}ethyl)-1H-1,2,3-triazol-4-ylmethyl Ester (33). For the preparation of **33**, **11** (582 mg, 1 mmol), CuSO$_4$·5H$_2$O (100 mg, 0.4 mmol, 40 mol %, in 1 mL of H$_2$O), sodium ascorbate (99 mg, 0.5 mmol, 50 mol %), and **25** (178 mg, 1 mmol) were subjected to the general procedure. After the mixture was stirred for 21 h, the reaction yielded **33** as a white foam (464 mg, 61%). Mp: 74 °C. HRMS-ESI: calcd for C$_{38}$H$_{42}$FN$_7$O$_9$ ([M + H]$^+$), 760.3101; found 760.3091. The purity of **33** was determined by analytical HPLC to be 99%, t_R = 8.63 ± 0.03 min (n = 3).

4-Fluoro-N-[1-(2-{2-[2-(2-{4-[2,4,6-trioxo-5-(4-phenoxyphenyl)hexahydropyrimidin-5-yl]piperazin-1-yl}-ethoxy)ethoxy]ethoxy}ethyl)-1H-1,2,3-triazol-4-ylmethyl]-benzenesulfonamide (34). For the preparation of **34**, **11** (349 mg, 0.6 mmol), CuSO$_4$·5H$_2$O (45 mg, 0.18 mmol, 30 mol %, in 0.5 mL of H$_2$O), sodium ascorbate (48 mg, 0.24 mmol, 40 mol %), and **26a** (128 mg, 0.6 mmol) were subjected to the general procedure. After the mixture was stirred for 18 h, the reaction yielded **34** as a colorless oil (128 mg, 27%). HRMS-ESI: calcd for C$_{37}$H$_{43}$FN$_8$O$_9$S ([M + H]$^+$), 795.2931; found 795.2939. The purity of **34** was determined by analytical HPLC to be 97%, t_R = 8.01 ± 0.01 min (n = 3).

4-Fluoro-N-methyl-N-[1-(2-{2-[2-(2-{4-[2,4,6-trioxo-5-(4-phenoxyphenyl)hexahydropyrimidin-5-yl]piperazin-1-yl}-ethoxy)ethoxy]ethoxy}ethyl)-1H-1,2,3-triazol-4-ylmethyl]-benzenesulfonamide (35). For the preparation of **35**, **11** (349 mg, 0.6 mmol), CuSO$_4$·5H$_2$O (45 mg, 0.18 mmol, 30 mol %, in 0.5 mL of H$_2$O), sodium ascorbate (48 mg, 0.24 mmol, 40 mol %), and **26b** (136 mg, 0.6 mmol) were subjected to the general procedure. After the mixture was stirred for 7.5 h, the reaction yielded **35** as a colorless oil (148 mg, 30%). HRMS-ESI: calcd for C$_{38}$H$_{45}$FN$_8$O$_9$S ([M + H]$^+$), 809.3087; found 809.3064. The purity of **35** was determined by analytical HPLC to be 98%, t_R = 8.51 ± 0.01 min (n = 3).

5-[4-(2-{2-[2-(2-{4-[4-(2-Fluoropyridin-3-yloxy)butyl]-1,2,3-triazol-1-yl}ethoxy)ethoxy]ethoxy}ethyl)piperazin-1-yl]-5-(4-phenoxyphenyl)pyrimidine-2,4,6-trione (36). For the preparation of **36**, **11** (291 mg, 0.5 mmol), CuSO$_4$·5H$_2$O (62 mg, 0.25 mmol, 50 mol %, in 0.5 mL H$_2$O), sodium ascorbate (59 mg, 0.3 mmol, 60 mol %), and **27** (106 mg, 0.55 mmol) were subjected to the general procedure. After the mixture was stirred for 5 h, the reaction yielded **36** as a light yellow wax (236 mg, 61%). HRMS-ESI: calcd for C$_{39}$H$_{47}$FN$_8$O$_8$ ([M + H]$^+$), 775.3574; found 775.3565. The purity of **36** was determined by analytical HPLC to be 99%, t_R = 8.30 ± 0.02 min (n = 3).

Radiochemistry. General Methods. Radiofluorinations were carried out on a modified PET tracer radiosynthesizer (TRACERLab Fx$_{FDG}$, GE Healthcare). The recorded data were processed by the TRACERLab Fx software (GE Healthcare). Separation and purification of the radiosynthesized compounds were performed on the following semipreparative radio-HPLC system: two K-1800 pumps and S-2500 UV detector (Knauer), GabiStar γ-detector (Raytest Isotopenmessgeräte GmbH) and an ACE-126-2510 column (250 mm × 10 mm). The recorded data were processed by the ChromGate HPLC software (Knauer). Radiochemical purities and specific activities were determined using an analytical radio-HPLC system composed of a Syknm S1021 pump, a Knauer K-2501 UV detector, a Crismatec NaI(TI) Scintibloc 51 SP51 γ-detector, a RP-HPLC Nucleosil 100-3 C-18 column (250 mm × 3 mm), and the GINA Star software (Raytest Isotopenmessgeräte GmbH). No-carrier-added aqueous [^{18}F]fluoride was produced on a RDS 111e cyclotron (CTI-Siemens) by irradiation of a 1.2 mL water target using 10 MeV proton beams on 97.0% enriched [^{18}O]water by the ^{18}O(p,n)^{18}F nuclear reaction. To recover the ^{18}O-water, the batch of aqueous [^{18}F]fluoride was passed through an anion exchange resin (Sep-Pak Light Waters Accell Plus

QMA cartridge, preconditioned with 5 mL of 1 M K$_2$CO$_3$ and 10 mL of water).

5-(4-{2-[2-(2-{2-[1-(2-[^{18}F]Fluoroethyl)-1H-1,2,3-triazol-4-ylmethoxy]ethoxy}ethoxy)ethoxy]ethyl}piperazin-1-yl)-5-(4-phenoxyphenyl)pyrimidine-2,4,6-trione ([^{18}F]30). No-carrier-added [^{18}F]fluoride (5.3−10.2 GBq) was eluted from a QMA-cartridge with a solution of Kryptofix 2.2.2 (18 mg) and K$_2$CO$_3$ (40 μL, 1 M) in acetonitrile/water (8:2, 1 mL). The aqueous solution was evaporated to dryness in vacuo. According to the procedure described by Glaser and Årstad,[32] 2-[^{18}F]fluoroethylazide was prepared by addition of 2-azidoethyl-4-methylbenzenesulfonate[31] (6 μL, 30 μmol) in anhydrous acetonitrile (0.3 mL) to the carefully dried [^{18}F]fluoride (potassium 222 cryptate) residue and subsequent reaction occurred at 84 °C for 15 min. After addition of acetonitrile (0.2 mL), 2-[^{18}F]fluoroethylazide was distilled at 120 °C under a flow of helium into a 5 mL flask containing DMF (0.5 mL) and cooled to 0 °C. The radiolabeling agent was collected with a radiochemical yield of 68 ± 8% (mean ± SD, decay corrected, n = 6). A solution of copper(II) sulfate pentahydrate (60 μL, 0.4 M), a solution of sodium ascorbate (50 μL, 0.6 M), water (600 μL), and a solution of **9** (7 mg, 12 μmol) in DMF (100 μL) were added. After 8 min at room temperature, the mixture was passed through a Waters Sep-Pak Light C18 cartridge filled with quartz wool. The cartridge was rinsed with DMF (0.3 mL), and the resulting mixture was evaporated to dryness in vacuo, followed by dissolving in acetonitrile/water (3:7, 1 mL, 0.1% TFA). An amount of 200 μL was fractionized by semipreparative radio-HPLC (conditions: λ = 254 nm; flow = 5.5 mL·min^{-1}; 33% CH$_3$CN in water (0.1% TFA) over 25 min). The product fraction of compound [^{18}F]30 was evaporated to dryness in vacuo and formulated in saline/ethanol (10:1, 0.5 mL) for further experimental use. The radioligand [^{18}F]30 was obtained in an overall radiochemical yield of 43 ± 9% (mean ± SD, decay-corrected, n = 6) in 140 min from end of radionuclide production. Radiochemical purities (>97%, t_R = 18.0 min) and specific radioactivities (11−20 GBq·μmol^{-1}) were determined by analytical radio-HPLC (conditions: λ = 254 nm; flow = 0.3 mL·min^{-1}; 33% CH$_3$CN in water (0.1% TFA)).

In Vitro Enzyme Inhibition Assays (Table 1). The inhibition potencies of barbituric acid derivatives **13**, **14**, and **28−36** against activated MMP-2, -8, -9, and -13 were assayed using the synthetic fluorgenic substrate (7-methoxycoumarin-4-yl)acetyl-Pro-Leu-Gly-Leu-(3-(2,4-dinitrophenyl)-L-2,3-diaminopropionyl)Ala-Arg-NH$_2$ (R&D Systems) as described previously.[30] In short, MMP-2, -8, -9, or -13 (each at 2 nM) and test compounds at varying concentrations (10 pM to 1 mM) in Tris-HCl (50 mM), pH 7.5, containing NaCl (0.2 M), CaCl$_2$ (5 mM), ZnSO$_4$ (20 μM), and 0.05% Brij 35 were preincubated at 37 °C for 30 min. An aliquot of substrate (10 μL of a 50 μM solution) was added to the enzyme−inhibitor mixture (90 μL), and the fluorescence changes were monitored using a Fusion universal microplate analyzer (Packard Bioscience) with excitation and emission wavelength of 330 and 390 nm, respectively. Reaction rates were measured from the initial 10 min and plotted as a function of inhibitor concentration. From the resulting inhibition curves, the IC$_{50}$ values were calculated by nonlinear regression analysis using the Grace 5.1.8 software (Linux).

Determination of Partition Coefficient (log $D_{7.4}$). The lipophilicity of radioligand [^{18}F]30 was assessed by determination of the water−octanol partition coefficient following a published procedure.[37] In brief, approximately 20 kBq [^{18}F]30 was mixed with equal amounts (0.5 mL) of PBS (pH 7.4) and 1-octanol and the resulting biphasic system was mixed vigorously for 1 min at room temperature. The tubes were centrifuged (3000 rpm, 2 min), and three samples of 100 μL of each layer were counted in a γ counter (Wallac Wizard, Perkin-Elmer Life Sciences). The partition coefficient was determined by calculating the ratio cpm(octanol)/cpm(PBS) and expressed as log $D_{7.4}$ (log(cpm$_{octanol}$/cpm$_{PBS}$)). Two independent experiments were performed in triplicate, and data were provided as mean values ± standard deviation.

Stability in Human Serum. The serum stability of radioligand [^{18}F]30 was evaluated by incubation in human serum at 37 °C for up to 120 min. An aliquot of the PBS-formulated ^{18}F-labeled compound (20 μL, 5 MBq) was added to a sample of human serum (200 μL), and

the mixture was incubated at 37 °C. Samples of 20 μL each were taken after periods of 10, 20, 30, 60, 90, and 120 min and quenched in methanol/CH_2Cl_2 (1:1 v/v, 100 μL) followed by centrifugation for 2 min. The organic layer was analyzed by analytical radio-HPLC (t_R = 6.5 min; analytical HPLC system II, linear gradient from 10% to 90% CH_3CN in water (0.1% TFA) over 9 min, followed by a linear gradient from 90% to 10% CH_3CN in water (0.1% TFA) over 6 min, 1.5 mL·min^{-1}).

In Vivo PET Studies. PET experiments were carried out using the high resolution (0.7 mm full width at half-maximum) quadHIDAC small-animal PET scanner (Oxford Positron Systems, Weston-on-the-Green, U.K.).[38] Balb/c mice (19–27 g) were anesthetized with isoflurane (1.5%/0.3 L min^{-1}) and placed on a heating pad to maintain body temperature for insertion of tail vein catheters (26G, BD VasculonPlus). The radiotracer [^{18}F]**30** (5–8 MBq in 100 μL, 150 μL saline flush) was injected 30 s after the start of acquisition. List-mode data were acquired for 60 min and reconstructed into dynamic time frames using an iterative resolution recovery reconstruction algorithm. Subsequently, the scanning bed was transferred to the CT scanner (Inveon, Siemens Medical Solutions, U.S.) and a CT acquisition with a spatial resolution of 80 μm was performed for each mouse. Reconstructed image data sets were co-registered based on extrinsic markers attached to the multimodal scanning bed and the image analysis software (Inveon Research Workplace 3.0, Siemens Medical Solutions, U.S.). Three-dimensional VOIs were defined over the respective organs in CT data sets, transferred to the co-registered PET data and analyzed quantitatively. Regional uptake was calculated as percentage of injected dose by dividing counts per milliliter in the VOI by total counts in the mouse multiplied by 100 (% ID/mL).

■ ASSOCIATED CONTENT

ⓈSupporting Information

Experimental procedures and analytical data for compounds **5**, **16–20**, **22**, **23** and ^{1}H, ^{13}C, and ^{19}F NMR data of compounds **28–36**. This material is available free of charge via the Internet at http://pubs.acs.org.

■ AUTHOR INFORMATION

Corresponding Author
*Phone: +492518347351. Fax: +498325147363. E-mail: kopka@uni-muenster.de.

■ ACKNOWLEDGMENTS

■ ABBREVIATIONS USED

CH, cyclohexane; CT, computed tomography; DMF, dimethylformamide; ECM, extracellular matrix; MMP, matrix metalloproteinase; MMPI, matrix metalloproteinase inhibitor; MT-MMP membrane-type matrix metalloproteinase; NBS, *N*-bromosuccinimide; PBS, phosphate buffered saline; PEG, polyethylene glycol; PET, positron emission tomography; RECK, reversion-inducing-cysteine-rich protein with kazal motifs; ROI, region of interest; SD, standard deviation; SPECT, single photon emission computed tomography; TEA, triethylamine; TEG, tetraethylene glycol; TFA, trifluoroacetic acid; THF, tetrahydrofuran; TIMP, tissue inhibitor of matrix metalloproteinases; TLC, thin layer chromatography; VOI, volume of interest

■ REFERENCES

(1) Folgueras, A. R.; Pendas, A. M.; Sanchez, L. M.; López-Otín, C. Matrix metalloproteinases in cancer: from new functions to improved inhibition strategies. *Int. J. Dev. Biol.* **2004**, *48*, 411–424.

(2) Overall, C. M.; López-Otín, C. Strategies for MMP inhibition in cancer: innovations for the post-trial era. *Nat. Rev. Cancer* **2002**, *2*, 657–672.

(3) Wagner, S; Breyholz, H.-J.; Faust, A.; Höltke, C.; Levkau, B.; Schober, O.; Schäfers, M; Kopka, K. Molecular imaging of matrix metalloproteinases in vivo using small molecule inhibitors for SPECT and PET. *Curr. Med. Chem.* **2006**, *13*, 2819–2838.

(4) Borkakoti, N. Structural studies of matrix metalloproteinases. *J. Mol. Med.* **2000**, *78*, 261–268.

(5) Stamenkovic, I. Extracellular matrix remodelling: the role of matrix metalloproteinases. *J. Pathol.* **2003**, *200*, 448–464.

(6) Rhee, J. S.; Coussens, L. M. ECKing MMP function: implications for cancer development. *Trends Cell Biol.* **2002**, *12*, 209–211.

(7) Vihinen, P.; Ala-aho, R.; Kahari, V. M. Matrix metalloproteinases as therapeutic targets in cancer. *Curr. Cancer Drug Targets* **2005**, *5*, 203–220.

(8) Newby, A. C. Dual role of matrix metalloproteinases (matrixins) in intimal thickening and atherosclerotic plaque rupture. *Physiol. Rev.* **2005**, *85*, 1–31.

(9) Tekabe, Y.; Li, Q.; Luma, J.; Weisenberger, D.; Sedlar, M.; Harja, E.; Narula, J.; Johnson, L. L. Noninvasive monitoring the biology of atherosclerotic plaque development with radiolabeled annexin V and matrix metalloproteinase inhibitor in spontaneous atherosclerotic mice. *J. Nucl. Cardiol.* **2010**, *17*, 1073–1081.

(10) Razavian, M.; Zhang, J.; Nie, L.; Tavakoli, S.; Razavian, N.; Dobrucki, L. W.; Sinusas, A. J.; Edwards, D. S.; Azure, M.; Sadeghi, M. M. Molecular imaging of matrix metalloproteinase activation to predict murine aneurysm expansion in vivo. *J. Nucl. Med.* **2010**, *51*, 1107–1115.

(11) Zhang, J.; Nie, L.; Razavian, M.; Ahmed, M.; Dobrucki, L. W.; Asadi, A.; Edwards, D. S.; Azure, M.; Sinusas, A. J.; Sadeghi, M. M. Molecular imaging of activated matrix metalloproteinases in vascular remodeling. *Circulation* **2008**, *118*, 1953–1960.

(12) Zheng, Q. H.; Fei, X.; Liu, X.; Wang, J. Q.; Stone, K. L.; Martinez, T. D.; Gay, D. J.; Baity, W. L.; Miller, K. D.; Sledge, G. W.; Hutchins, G. D. Comparative studies of potential cancer biomarkers carbon-11 labeled MMP inhibitors (*S*)-2-(4'-[^{11}C]methoxybiphenyl-4-sulfonylamino)-3-methylbutyric acid and *N*-hydroxy-(*R*)-2-{[(4'-[^{11}C]methoxyphenyl)sulfonyl]benzylamino}-3-methylbutanamide. *Nucl. Med. Biol.* **2004**, *31*, 77–85.

(13) Grams, F.; Brandstetter, H.; D'Alo, S.; Geppert, D.; Krell, H. W.; Leinert, H.; Livi, V.; Menta, E.; Oliva, A.; Zimmermann, G. Pyrimidine-2,4,6-triones: a new effective and selective class of matrix metalloproteinase Inhibitors. *Biol. Chem.* **2001**, *382*, 1277–1285.

(14) Maquoi, E.; Sounni, N. E.; Devy, L.; Olivier, F.; Frankenne, F.; Krell, H.-W.; Grams, F.; Foidart, J.-M.; Noël, A. Anti-invasive, antitumoral, and antiangiogenic efficacy of a pyrimidine-2,4,6-trione derivative, an orally active and selective matrix metalloproteinase inhibitor. *Clin. Cancer Res.* **2004**, *10*, 4038–4047.

(15) Breyholz, H.-J.; Schäfers, M.; Wagner, S.; Höltke, C.; Faust, A.; Rabeneck, H.; Levkau, B.; Schober, O.; Kopka, K. C-5-disubstituted barbiturates as potential molecular probes for noninvasive matrix metalloproteinase imaging. *J. Med. Chem.* **2005**, *48*, 3400–3409.

(16) Wagner, S.; Breyholz, H. J.; Law, M. P.; Faust, A.; Höltke, C.; Schröer, S.; Haufe, G.; Levkau, B.; Schober, O.; Schäfers, M.; Kopka, K. Novel fluorinated derivatives of the broad-spectrum MMP inhibitors *N*-hydroxy-2(*R*)-{[(4-methoxyphenyl)sulfonyl](benzyl)- and (3-picolyl)-amino}-3-methyl-butanamide as potential tools for

the molecular imaging of activated MMPs with PET. *J. Med. Chem.* **2007**, *50*, 5752−5764.

(17) Kopka, K.; Breyholz, H.-J.; Wagner, S.; Law, M. P.; Riemann, B.; Schröer, S.; Trub, M.; Guilbert, B.; Levkau, B.; Schober, O.; Schäfers, M. Synthesis and preliminary biological evaluation of new radioiodinated MMP inhibitors for imaging MMP activity in vivo. *Nucl. Med. Biol.* **2004**, *31*, 257−267.

(18) Schäfers, M.; Riemann, B.; Kopka, K.; Breyholz, H.-J.; Wagner, S.; Schäfers, K. P.; Law, M. P.; Schober, O.; Levkau, B. Scintigraphic imaging of matrix metalloproteinase activity in the arterial wall in vivo. *Circulation* **2004**, *109*, 2554−2559.

(19) Brandstetter, H.; Grams, F.; Glitz, D.; Lang, A.; Huber, R.; Bode, W.; Krell, H. W.; Engh, R. A. The 1.8-Å crystal structure of a matrix metalloproteinase-8 barbiturate inhibitor complex reveals a peviously unobserved mechanism for collagenase substrate recognition. *J. Biol. Chem.* **2001**, *276*, 17405−17412.

(20) Tochowicz, A.; Maskos, K.; Huber, R.; Oltenfreiter, R.; Dive, V; Yiotakis, A.; Zanda, M.; Bode, W.; Goettig, P. Crystal structures of MMP-9 complexes with five inhibitors: contribution of the flexible Arg424 side-chain to selectivity. *J. Mol. Biol.* **2007**, *371*, 989−1006.

(21) Breyholz, H.-J.; Wagner, S.; Faust, A.; Riemann, B.; Höltke, C.; Hermann, S.; Schober, O.; Schäfers, M.; Kopka, K. Radiofluorinated pyrimidine-2,4,6-triones as molecular probes for noninvasive MMP-targeted imaging. *ChemMedChem* **2010**, *5*, 777−789.

(22) Zang, W.; Kung, M. P.; Oya, S.; Hou, C.; Kung, H. F. 18F-labeled styrylpyridines as PET agents for amyloid plaque imaging. *Nucl. Med. Biol.* **2007**, *34*, 89−97.

(23) Wu, Z.; Li, Z. B.; Chen, K.; Cai, W.; He, L.; Chin, F. T.; Li, F.; Chen, X. MicroPET of tumor integrin $\alpha_\nu\beta_3$ expression using 18F-labeld PEGylated tetrameric RGD peptide (18F-FPRGD4). *J. Nucl. Med.* **2007**, *48*, 1536−1544.

(24) Chen, X.; Park, R.; Hou, Y.; Khankaldyyan, V.; Gonzales-Gomez, I; Tohme, M; Bading, J. R.; Laug, W. E.; Conti, P. S. MicroPet imaging of brain tumor angiogenesis with 18F-labeled PEGylated RGD peptide. *Eur. J. Nucl. Med. Mol. Imaging* **2004**, *31*, 1081−1089.

(25) Faust, A.; Waschkau, B.; Waldeck, J.; Höltke, C.; Breyholz, H.-J.; Wagner, S.; Kopka, K.; Heindel, W.; Schäfers, M.; Bremer, C. Synthesis and evaluation of a novel fluorescent photoprobe for imaging matrix metalloproteinases. *Bioconjugate Chem.* **2008**, *19*, 1001−1008.

(26) Hutchings, S.; Liu, W.; Radinov, R. Palladium-catalyzed arylation of diisopropyl malonate applied to the efficient synthesis of the selective MMP inhibitor 5-(4-phenoxyphenyl)-5-[4-(2-pyrimidinyl)-1-piperazinyl]barbituric acid. *Heterocycles* **2006**, *67*, 763−768.

(27) Tahtaoui, C.; Parrot, I.; Klotz, P.; Guillier, F.; Galzi, J.-L.; Hilbert, M.; Ilien, B. Fluorescent pirenzepine derivatives as potential bitopic ligands of the human M1 muscarinic receptor. *J. Med. Chem.* **2004**, *47*, 4300−4315.

(28) Vaidyanathan, G.; Zalutsky, M. R. Labeling proteins with fluorine-18 using N-succinimidyl 4-[18F]fluorobenzoate. *Nucl. Med. Biol.* **1992**, *19*, 275−281.

(29) Rostovtsev, V.; Green, L. G.; Fokin, V. V.; Sharpless, K. B. A stepwise Huisgen cycloaddition process: copper(I)-catalyzed regioselectoive "ligation" of azides and terminal alkynes. *Angew. Chem.* **2002**, *114*, 2708−2711; *Angew. Chem., Int. Ed.* **2002**, *41*, 2596−2599.

(30) Huang, W.; Meng, Q.; Suzuki, K.; Nagase, H.; Brew, K. Mutational study of the amino-terminal domain and human tissue inhibitor of metalloproteinases 1 (TIMP-1) locates an inhibitory region for matrix metallo proteinases. *J. Biol. Chem.* **1997**, *272*, 22086−22091.

(31) Demko, Z. P.; Sharpless, K. B. An intramolecular [2+3] cycloaddition route to fused 5-heterosubstituted tetrazoles. *Org. Lett.* **2001**, *3*, 4091−4094.

(32) Glaser, M.; Arstad, E. "Click labeling" with 2-[18F]fluoroethylazide for positron emission tomography. *Bioconjugate Chem.* **2007**, *18*, 989−993.

(33) Vaidyanathan, G.; White, B. J.; Zalutsky, M. R. Propargyl 4-[18F]fluorobenzoate: a putatively more stable prosthetic group for the fluorine-18 labeling of biomolecules via click chemistry. *Curr. Radiopharm.* **2009**, *2*, 63−74.

(34) Ramenda, T.; Kniess, T.; Bergmann, R.; Steinbach, J.; Wuest, F. Radiolabelling of proteins with fluorine-18 via click chemistry. *Chem. Commun.* **2009**, *48*, 7521−7523.

(35) Prante, O.; Tietze, R.; Hocke, C.; Löber, S.; Hübner, H.; Kuwert, T.; Gmeiner, P. Synthejkjhmjhvhmnhmsis, radiofluorination and in vitro evaluation of pyrazolo[1,5-a]pyridine based dopamine D4 receptor ligands: discovery of an inverse agonist radioligand for PET. *J. Med. Chem.* **2008**, *51*, 1800−1810.

(36) Inkster, J. A. H.; Guérin, B.; Ruth, T. J.; Adam, M. J. Radiosynthesis and bioconjugation of [18F]FPy5yne, a prosthetic group for the 18F labeling of bioactive peptides. *J. Labelled Compd. Radiopharm.* **2008**, *51*, 444−452.

(37) Prante, O.; Hocke, C.; Löber, S.; Hübner, H.; Gmeiner, P.; Kuwert, T. Tissue distribution of radioiodinated FAUC113: assessment of a pyrazolo[1,5-a]pyridine-based dopamine D4 receptor radioligand candidate. *Nuklearmedizin* **2006**, *45*, 41−48.

(38) Schäfers, K. P.; Reader, A. J.; Kriens, M.; Knoess, C.; Schober, O.; Schäfers, M. Performance evaluation of the 32-module quadHIDAC small-animal PET scanner. *J. Nucl. Med.* **2005**, *46*, 996−1004.